Polymer 50 (2009) 3007–3015

Contents lists available at ScienceDirect

Polymer

journal homepage: www.elsevier.com/locate/polymer

The effect of microstructure on the rate-dependent stress–strain behavior of poly(urethane urea) elastomers

Sai S. Sarva [a], Alex J. Hsieh [a,b,*]

[a] Institute for Soldier Nanotechnologies, Massachusetts Institute of Technology, 500 Technology Square, Cambridge, MA 02139, USA
[b] U.S. Army Research Laboratory, AMSRD-ARL-WM-MD, Aberdeen Proving Ground, MD 21005-5069, USA

ARTICLE INFO

Article history:
Received 8 April 2009
Accepted 11 April 2009
Available online 23 April 2009

Keywords:
Poly(urethane urea) elastomers
Phase mixing
Rate sensitivity

ABSTRACT

Segmented poly(urethane urea) materials (PUUs) exhibit versatile mechanical properties and have drawn great interest due to their potential for protection against projectile impacts and blast loadings. To optimize the performance of PUUs for various high rate applications, specific features of their mechanical behavior have to be suitably tailored by altering the microstructure. Hence the micromechanisms governing the mechanical behavior must be identified, understood and leveraged. In this study, the effects of varying microstructure on the rate-dependent mechanical behavior were examined for select PUU materials. As expected, increasing the hard segment content increased the stiffness and the flow stress levels. Interestingly, it was observed that promoting phase mixing among the hard and soft segment domains of the PUU material greatly enhanced its rate-dependent stiffening and strain hardening behavior. These insights can help design PUUs for articles that manifest improved protective abilities under impact, while maintaining their flexibility during normal use. The potential applications for such materials are extensive, including face masks and goggles, which require excellent folding/un-folding capabilities, while also providing superior impact resistance.

Published by Elsevier Ltd.

1. Introduction and background

Segmented poly[urethane urea] (PUU) elastomers, like polyurethane (PU) based materials, exhibit versatile mechanical properties making them an excellent choice for various structural applications in the form of films, fibers, adhesives and coatings. The chemical structure of a PUU generally consists of long-chain polyols and diisocyanates connected with short-chain diamines, which are used as chain extenders. The long-chain polyols and diisocyanates form soft segments with urethane linkages, whereas the short-chain diamines react with diisocyanates to form hard segments with urea linkages. Microphase separation resulting from the thermodynamic incompatibility between the hard and soft segments gives rise to a broad range of physical and mechanical properties [1]. The choice of diisocyanates, long-chain polyols and chain extenders greatly affects the ability of the soft and hard segments to crystallize, as well as to microphase separate, and hence is crucial to tailoring of the microstructures and the resulting macroscopic properties of these elastomers [1].

Previously, studies have been conducted to examine the microstructures of similar segmented elastomers. Aneja and Wilkes [2] examined the nanoscale morphology for a series of segmented PUs containing monodisperse hard segments with one, two, three and four repeating units. These polymers were based on 1,4-butanediol extended piperazine hard segments with poly(tetramethylene oxide), PTMO, soft segments. Phase images obtained by atomic force microscopy (AFM) were the first to reveal spatially resolved features such as dimensions, shape and interconnectivity of the hard segment (HS) domains. They observed a spherulitic morphology for the HS domains, similar to that previously reported through small-angle light scattering and scanning electron microscopy [3]. They also observed that the crystalline hard segments preferentially orient along tangential directions to the spherulites, and that the HS domain interconnectivity grows with increasing HS content.

The deformation mechanisms of PUs and PUUs have also been reported in literature. These investigations of microstructural changes were generally based on simultaneous mechanical testing coupled with techniques such as wide-angle X-ray diffraction, small-angle X-ray scattering and time-resolved Fourier transform infrared spectroscopy [4,5]. With increasing deformation, observations have been reported of rotation and orientation of HS lamellar domains towards the axis of elongation, along with

* Corresponding author. U.S. Army Research Laboratory, AMSRD-ARL-WM-MD, Aberdeen Proving Ground, MD 21005-5069, USA. Tel.: +1 410 306 0698; fax: +1 410 306 0806.
E-mail address: ahsieh@arl.army.mil (A.J. Hsieh).

0032-3861/$ – see front matter Published by Elsevier Ltd.
doi:10.1016/j.polymer.2009.04.025

stretching and shearing of the soft segment (SS) chains. At very large strains (300–500%), the HS domains were observed to breakup and restructure to form fibrils [5]. It is now well known that the thermal, physical and mechanical properties of PUs and PUUs are governed by their microphase-separated morphology [6–15]. Abouzahr et al. [6] studied the effects of composition on the morphology, tensile stress–strain behavior and hysteresis of segmented PUs comprising of PTMO, 4,4′-diphenylmethane diisocyanate, MDI, and butanediol. At high HS concentrations, domain disruption was prevalent even at low levels of elongation and the irreversible re-structuring of the morphology led to a high hysteresis in these materials. PUs possessing domain structures that were distinct and not interconnected displayed the most desirable elastomeric properties such as high elongations and low hysteresis. Sheth et al. [13] systematically evaluated the influence of SS molecular weight, HS content and the chain extender type on the dynamic mechanical behavior of 4,4′-dicyclohexylmethane diisocyanate (HMDI)–polydimethylsiloxane (PDMS) based PUs and PUUs. Their results showed that the molecular weight of PDMS and the length and symmetry of the chain extenders (diols for urethanes and diamines for ureas) had a marked effect on the morphology, the rubbery plateau modulus and the tensile behavior of both PU and PUU materials. Generally, it was observed that the degree of microphase separation and the values of rubbery plateau and tensile modulus were significantly greater in the PUU than in the corresponding PU. This was attributed to a difference in the cohesive strengths of the bidentate in urea versus the monodentate in urethane.

The overall rate-dependent mechanical behaviors of PUs and polyureas have also been studied. Qi and Boyce [15] examined the compressive stress–strain behavior, including the nonlinear hyperelastic behavior, time dependence, hysteresis, and softening of a segmented PU. They also developed a physically-based constitutive model to capture various features of the mechanical behavior; an excellent agreement between the experimental results and the model predictions was demonstrated. Boyce and co-workers [16,17] have also examined the high strain rate compressive behavior of PUs and a polyurea. As the strain rate was increased, the stress–strain behaviors were observed to transition from a rubbery type behavior to a leathery or a glassy type behavior. The transitions in their stress–strain behaviors were directly associated with the rate-dependent shifts in their viscoelastic behaviors observed through dynamic mechanical analysis. Their studies of PUs indicated that incorporation of dimethyl propanediol (DMPD) as a chain extender resulted in greater strain rate sensitivity in comparison to the incorporation of butanediol (BDO); as the strain rate was increased from 10^{-3} to 10^{4} s^{-1}, the initially rubbery-like DMPD-containing PU transitioned to a distinctly glassy type behavior. Hsieh et al. [18] examined the fold recovery behavior[1] of the same PUs by bending PU films at 180° and measuring their elastic recovery over time. It was observed that the DMPD-containing PU which had a ~50 °C greater glass transition temperature, exhibited a large reduction in fold/flexural recovery in comparison to the PUs with BDO, which were able to recover rapidly and completely after being released from bending.

Understanding the very high strain rate mechanical behavior is critical for the design of segmented PUs and PUUs, particularly for use in composite structures against projectile or blast impacts [19–21]. Bogoslow et al. [20] demonstrated that elastomers can provide increased energy dissipation through a mechanism of strain-induced transition from a rubbery to glassy state. Impact testing of polybutadiene-based polyurea, backed by steel plates showed a transition to glassy state causing a brittle failure mode and increasing the energy dissipation in comparison to polybutadiene rubber, which remained rubbery during impact. The segmental dynamics of the polybutadiene rubber determined through dielectric spectroscopic measurements were almost three orders of magnitude faster than those for polybutadiene-based polyurea [20]. Hence the polybutadiene rubber chains were able to accommodate the impact and respond in a rubbery mode since the frequency of segmental relaxation required to transition them to a glassy state under ambient conditions of temperature and pressure was more than three orders of magnitude greater than the strain rate of impact ($\sim 10^{5}$ s^{-1}). On the other hand, similar impact caused a transition to a glassy state in the polybutadiene-based polyurea due to its much slower local segmental dynamics, resulting in increased energy dissipation but a brittle mode of failure.

The objective of the present research is to gain a better understanding of the micromechanisms governing the mechanical behavior of segmented PUUs over a range of loading conditions. Of particular interest is the ability to design materials that are flexible, exhibit good fold/flexural recovery after storage and provide superior impact resistance; fold recovery capabilities are essential for applications such as face mask protective systems that are used by first response and special force operations [22]. Here we examine a set of model PUU materials and aim to elucidate the effects of composition, including the HS content and the molecular weight of the PTMO soft segment on the morphology, viscoelastic behavior and the rate-dependent mechanical behavior. Results obtained through characterization techniques, including small-angle X-ray scattering (SAXS), differential scanning calorimetry (DSC), and dynamic mechanical analysis (DMA) are used to correlate with and analyze the stress–strain data of these PUUs over a broad range of strain rates.

2. Materials synthesis

Poly(urethane urea) materials with varying hard segment (HS) content were chosen for use in this study. Additionally, for one of the PUU compositions, the molecular weight of the soft segment poly(tetramethylene oxide), a polyether diol, was varied from 2000 to 1000 g/mol. These PUU materials were synthesized from 4,4′-dicyclohexylmethane diisocyanate (HMDI -Desmodur W, Bayer MaterialScience), poly(tetramethylene oxide) (PTMO-PolyTHF, BASF Corporation), and a chain extender, diethyltoulenediamine (DETA-Ethacure® 100-LC, Albemarle Corporation, Baton Rouge, Louisiana) [23].

The PUU compounds were prepared following a two-step, pre-polymer synthesis method. First, to prepare the pre-polymer, the HMDI was weighed and heated to 65 °C in a dried round-bottomed flask in a nitrogen environment. Separately, the PTMO was accurately weighed and mixed thoroughly with a tin catalyst in another container and the mixture was then held at 45–50 °C. The PTMO/tin mixture was then added to the HMDI and blended with the help of a standard laboratory scale mechanical overhead stirrer, during which the exotherm temperature reached a peak value of nearly 120 °C. After the exotherm subsided, the mixture was heated in an external oil bath and held at 130–135 °C for several hours. The reaction mixture was then cooled and allowed to stand overnight at room temperature. Next, prior to the PUU synthesis, the pre-polymer was heated to 150 °C for a minimum of 30 min, and then cooled down to 65 °C while being slowly stirred and degassed in

[1] There is no experimental protocol that is extensively used to characterize elastomers under such conditions. Even though there exists an ASTM 3768 – 06 standard for testing the flexural recovery of urethanes, currently in most circumstances these tests are performed under conditions that are relevant to the target applications.

a vacuum chamber. This pre-polymer was then reacted with the DETA. Since the resulting reaction was extremely rapid, the pre-weighed DETA was introduced into the pre-polymer using a syringe, followed by a thorough and rapid mixing, further followed by degassing for ~1 min. The resulting mixture was then poured into molds to form plaques of the requisite thickness, and cured overnight at 110 °C.

Table 1 lists the compositions of the four different PUU materials chosen for evaluation in this study. In the sample nomenclature, the numerals '*x*–*y*–*z*' refer to the molar ratio of diisocyanate: diamine chain extender:PTMO, and the succeeding '1k' or '2k' refers to the molecular weight of PTMO as either 1000 or 2000 g/mol, respectively. The material nomenclatured '2-1-1 2k' was selected as the baseline formulation. The HS contents (%HS) noted in Table 1 were calculated using an approach based on the urea content, as described by the below equation [10]:

$$\%\mathrm{HS} = \frac{100(R-1)(M_{\mathrm{di}}+M_{\mathrm{da}})}{(M_{\mathrm{g}}+R(M_{\mathrm{di}})+(R-1)(M_{\mathrm{da}}))} \quad (1)$$

where R is the molar ratio of the diisocyanate to PTMO, and M_{di}, M_{da} and M_{g} are the number average molecular weights of the diisocyanate, diamine and PTMO, respectively. Equation (1) accounts only for the portion of diisocyanate that reacts with diamine and hence, it primarily represents the material residing in the hard domains [10]. The experimental results described in the following sections will be examined in correlation with the HS content values noted here.

3. Materials characterization

3.1. Experimental techniques

3.1.1. Small-angle X-ray scattering (SAXS)

The influence of composition on the microstructure of the PUUs was examined via small-angle X-ray scattering. Measurements were made with a customized 3 m pinhole collimated SAXS camera. A Rigaku Ultrax18 rotating anode with a copper target was operated at 40 kV/60 mA to generate X-rays with $\lambda = 1.5418$ Å. Two dimensional data sets were collected using a Molecular Metrology 2D multi-wire area detector placed ~65 cm from the sample. The data were azimuthally averaged and corrected for air scatter and detector anomalies. The location of the scattering maximum corresponds to the average periodic spatial resolution between the microdomains, and the average interdomain spacing '*d*' is estimated using Bragg's law as:

$$q = 4\pi \sin\theta/\lambda = 2\pi d \quad (2)$$

where 'q' is the scattering vector, 'λ' is the wavelength of the incident radiation and 'θ' is one half the scattering angle.

3.1.2. Differential scanning calorimetry

The effects of HS content and SS molecular weight on the thermal transitions were examined by differential scanning calorimetry (DSC). Measurements were performed using a TA Instruments Q1000 differential scanning calorimeter. PUU samples of 5–8 mg weight were heated at 10 °C/min over a temperature range of −90 to 250 °C.

3.1.3. Dynamic mechanical analysis (DMA)

DMA testing was carried out using a TA Instruments Q800 DMA in tension mode. Rectangular specimens with dimensions of 3 mm width, 2 mm thickness and 12 mm gauge length were used. Tests were conducted at frequencies of 1, 10 and 50 Hz, using a constant strain amplitude of 0.1%, for a temperature range of −150 to 200 °C at a ramp rate of 3 °C/min.

3.2. Characterization results

3.2.1. Small-angle X-ray scattering (SAXS)

Fig. 1 compares the scattering intensities for the four materials, exhibiting the effects of varying the HS content and the SS molecular weight (MW). The base material, PUU 2-1-1 2k, exhibits a broad scattering peak with an average interdomain spacing of ~15.9 nm, suggesting the presence of isolated HS domains as is typically observed in microphase-separated PUUs. For the series of PUU 2k samples (i.e. with the PTMO MW being maintained the same), the intensity of the scattering peak successively increases when the 2-1-1 2k, 3-2-1 2k and 4-3-1 2k materials are compared. This can be attributed to the increase in scattering contrast between the HS domains and the SS regions, with increasing HS content. In comparison to the 2-1-1 2k, the scattering peak of the 3-2-1 2k is observed to shift to a smaller angle, indicating an increase in the average interdomain spacing due to a growth in the HS domain size. As the HS content is further increased, the scattering peak for the 4-3-1 2k grows in intensity, but becomes relatively broad and indistinct. This lack of a pronounced scattering peak at high HS contents, as previously observed by Abouzahr et al. [6], could result either from an emergence of growingly irregular shape of the HS domains or from an onset of a significant change in the morphology, such as an increased interconnectivity of HS domains.

The scattering characteristics also differ when the molecular weight of the soft segment is varied. Fig. 1 shows that the scattering

Table 1
Compositions and the HS contents of the synthesized PUU materials.

	Molar ratio of diisocyanate: chain extender:PTMO	MW of PTMO (g/mol)	Hard Segment Content (wt%)
PUU 2-1-1 2k	2:1:1	2000	16.3
PUU 3-2-1 2k	3:2:1	2000	28.0
PUU 4-3-1 2k	4:3:1	2000	36.9
PUU 2-1-1 1k	2:1:1	1000	25.9

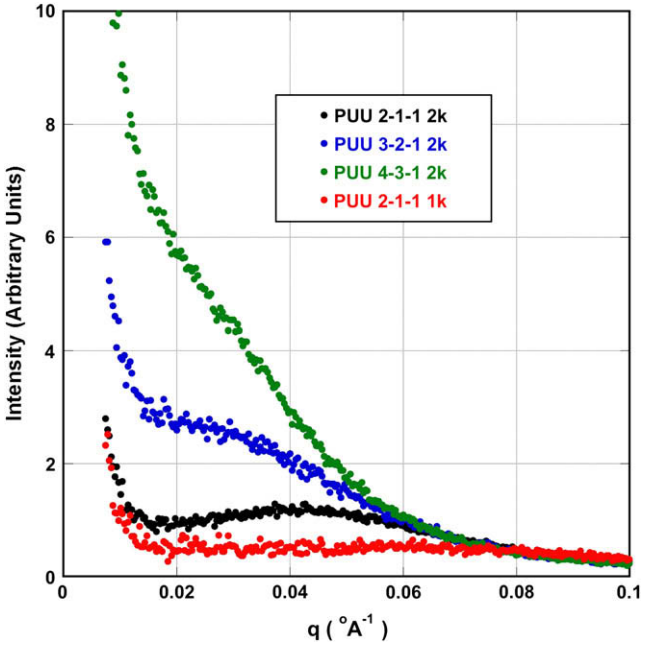

Fig. 1. SAXS data for the various samples. (For interpretation of the references to colour in this figure legend, the reader is referred to the web version of this article.)

peak for the PUU 2-1-1 1k material is located at a comparatively large angle and exhibits a significantly decreased intensity. The peak location for the PUU 2-1-1 1k corresponds to an average interdomain spacing of ~11.4 nm. Keeping the molar ratio the same, a reduction in the SS molecular weight from 2000 g/mol to 1000 g/mol results in a smaller SS content, which contributes to the decrease in the HS interdomain spacing. Additionally, the scattering peak for the PUU 2-1-1 1k exhibits a significantly reduced intensity indicating a lowered X-ray contrast, in comparison to the PUU 3-2-1 2k which has similar HS/SS content. The SS content remaining the same, the molar content of the SS hydroxyl groups in the PUU 2-1-1 1k is twice that of the PUU 3-2-1 2k. Hence a greater number of isocyanate groups are required for reactions with the greater number of SS diols in the PUU 2-1-1 1k due to stoichiometric requirements. As a result, the molar content of the urethane linkages connecting the soft segments within the SS domains in the PUU 2-1-1 1k is approximately twice that in the PUU 3-2-1 2k. This leads to an increase in the intermolecular interactions, via hydrogen bonds between the hard and the soft segments, and a greater phase mixing.

3.2.2. Differential scanning calorimetry

Fig. 2A shows the DSC curves for the three PUU 2k materials, which exhibit both the SS glass transitions ($T_{g,s}$) and the HS glass transitions ($T_{g,h}$). The precise $T_{g,s}$ locations were determined via dynamic mechanical analysis (see Section 3.2.3). No evidence of melting endotherms, associated with melting of either crystalline SS or HS domains was observed. Note that for the same samples, wide angle X-ray scattering (WAXS) data showed only a broad halo with a Bragg spacing of ~4.4 Å, confirming the amorphous nature of these PUU samples [24]. Fig. 2A also shows that for the PUU 2k samples, as the HS content is increased, the $T_{g,h}$ becomes increasingly distinct. In addition, the step change in heat flow, reflecting the specific heat change from below to above the $T_{g,h}$, is significantly larger in the PUU 3-2-1 2k and the PUU 4-3-1 2k than in the PUU 2-1-1 2k, which indicates the emergence of HS domains with greater HS content.

Fig. 2B compares the PUU 2-1-1 1k material with the PUU 3-2-1 2k (among the 2k materials, the 3-2-1 2k was chosen for comparison since its HS content is similar to that of the 2-1-1 1k). The 2-1-1 1k exhibits a broadening of the $T_{g,s}$, with a noticeable shift to a higher temperature. Also its $T_{g,h}$ has shifted to a lower temperature, thus bringing the two (soft and hard segment) glass transitions closer, suggesting a greater phase mixing in the PUU 2-1-1 1k than in the PUU 2k samples. This observation also corroborates the SAXS data. Note that the $T_{g,h}$ peaks exhibit shoulders at ~150 °C, which are associated with the phase mixed HS content and signify the onset of the transition.

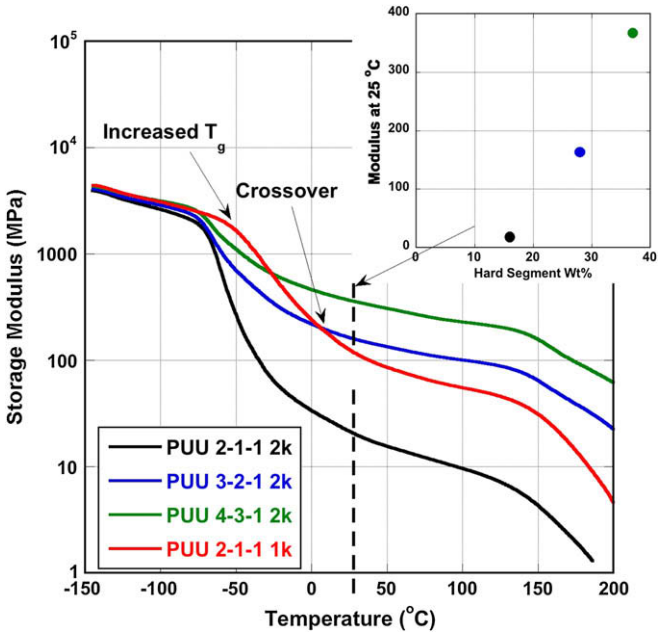

Fig. 3. DMA storage moduli curves at 1 Hz for the various PUU materials. Inset shows the effect of HS content on the rubbery plateau modulus of the PUU 2k materials at 25 °C.

3.2.3. Dynamic mechanical analysis (DMA)

3.2.3.1. Effect on the storage modulus. Fig. 3 shows the storage moduli curves for the PUU materials at 1 Hz frequency. The curve for the base material, PUU 2-1-1 2k, shows that when the temperature is surpassed at approximately −75 °C, the onset of SS mobility results in a very drastic decline in the modulus (a drop of over two orders of magnitude) until the rubbery plateau is eventually reached. The storage moduli curves for the PUU 2k materials show a considerable increase in the rubbery plateau modulus with increasing HS content. To quantify this effect, the magnitudes of the

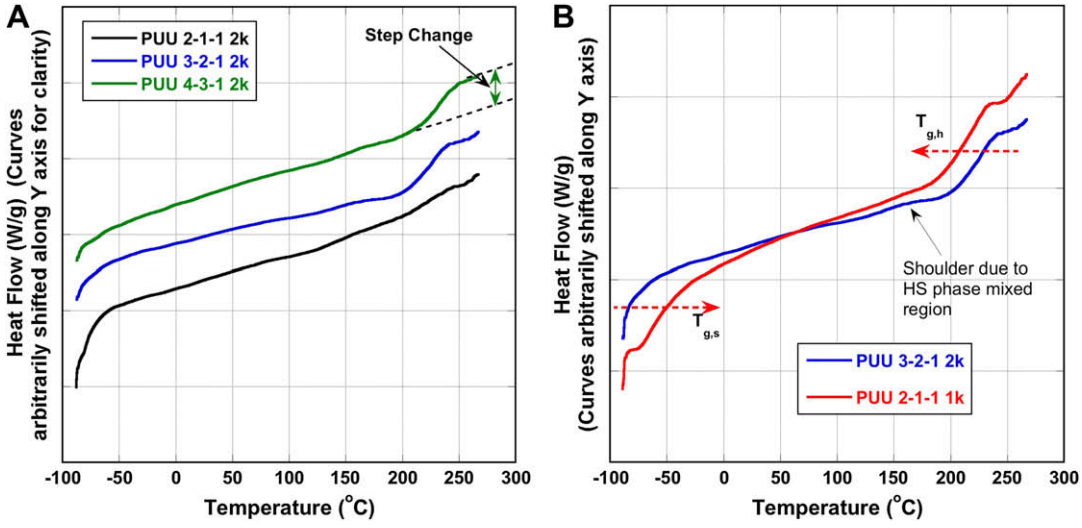

Fig. 2. (A) DSC thermograms for PUU 2k samples (B) Shift of $T_{g,s}$ and $T_{g,h}$ towards each other in PUU 2-1-1 1k.

Table 2
The values of rubbery plateau modulus, E', determined at 25 °C.

	E' at 25 °C (MPa)
PUU 2-1-1 2k	18
PUU 3-2-1 2k	163
PUU 4-3-1 2k	367
PUU 2-1-1 1k	126

rubbery plateau moduli were determined at a temperature of 25 °C; these are listed in Table 2 and also shown in the inset of Fig. 3. A very strong dependence of the rubbery plateau modulus on the HS content is observed. The modulus rises from 18 MPa for the 2-1-1 2k material with a 16.3% HS content to 367 MPa for the 4-3-1 2k material with a 36.9% HS content. Similar strong, nonlinear dependence of the elastic modulus on the HS content was also observed by Abouzahr et al. [6] in their studies of stress–strain behavior of PUs. They attribute this to morphological changes that arise at high HS contents, such as the interlocking of the HS domains.

Additionally, the SS molecular weight significantly alters the nature of the storage modulus curve. In comparison to the 3-2-1 2k, the 2-1-1 1k material exhibits a significant difference in its curve (note again that though 2-1-1 2k was the base formulation for the 2k materials, when comparing the effect of the SS molecular weight, we compare the properties of the 3-2-1 2k with the 2-1-1 1k due to their similar HS contents). At 25 °C, the rubbery plateau modulus for the 2-1-1 1k material is lower, but as the temperature is decreased, its storage modulus rises at a faster rate and at ~5 °C, it crosses over with the 3-2-1 2k material. By −50 °C, the 2-1-1 1k has a significantly greater modulus than the 3-2-1 2k. This change in shape of the storage modulus curve for the 2-1-1 1k material is caused due to its $T_{g,s}$ being located at a higher temperature, which is a result of the greater phase mixing in this material. In polymers, the lowering of the temperature is equivalent to increasing the strain rate [25,26]. These storage moduli curves demonstrate that though the 2-1-1 1k material is more compliant than the 3-2-1 2k at lower strain rates (higher temperatures), it will be significantly stiffer than the 3-2-1 2k at higher strain rates (lower temperatures).

3.2.3.2. Effect on the soft segment glass transition. The precise $T_{g,s}$ locations for the PUU materials were determined from the DMA loss modulus data; see Table 3. For the PUU 2k samples, the change in the HS content did not exhibit any significant effect on the $T_{g,s}$ location. However, the increase in the HS content was accompanied by a substantial decrease in the loss factor (tan δ) intensity. Fig. 4 shows the tan δ curves obtained at a frequency of 1 Hz for the PUU 2k samples. As the HS content is increased, the number of physical crosslinks that is available to restrict the SS chain mobility also increases and hence the tan δ intensity, which characterizes the damping behavior, successively decreases. For the 4-3-1 2k material, the intensity is almost one half the intensity for the 2-1-1 2k material, indicating a greatly reduced damping behavior. These materials exhibit multiple relaxation peaks, associated with the $T_{g,s}$ in the −75 °C and 50 °C range. The 2-1-1 2k material exhibits a very distinct and intense peak at −64 °C along with a weaker shoulder at 21 °C. The more intense and dominant peak relates to the relaxation of the SS rich phase and the weaker shoulder presumably relates to the SS phase mixed regions [27]. As the HS content is increased, the dominant tan δ peak becomes less distinct. Also, two separate peaks are seen to emerge from the dominant peak for the 3-2-1 2k and 4-3-1 2k materials. Further characterization of these multiple SS relaxation peaks is currently in progress.

Table 3
Values of $T_{g,s}$ determined from DMA for the PUU samples.

	$T_{g,s}$ (°C) obtained using DMA loss modulus data at a frequency of		
	1 Hz	10 Hz	50 Hz
PUU 2-1-1 2k	−64	−60	−58
PUU 3-2-1 2k	−67	−62	−60
PUU 4-3-1 2k	−67	−64	−59
PUU 2-1-1 1k	−44	−37	−33

Variation in the SS molecular weight also has a great effect on the $T_{g,s}$. The $T_{g,s}$ for the PUU 2-1-1 1k is ~20 °C higher than that for the PUU 2k materials (see Fig. 4 and Table 3); note that this increase in $T_{g,s}$ for the PUU 2-1-1 1k was also observed in the DSC data. Also, the nature of the tan δ peaks for the 2k materials is vastly different than that for the PUU 2-1-1 1k material. The PUU 2-1-1 1k displays a single broad tan δ peak, which appears to be a result of the merging of the multiple SS relaxation peaks that were observed in the 2k materials. This is likely due to a change in morphology as a result of the greater phase mixing in the PUU 2-1-1 1k material.

3.2.3.3. Effect on the rate dependency. Recently, it has been demonstrated that the rate-sensitive mechanical behavior of polymeric materials is directly associated with the rate/frequency dependent shifts in their viscoelastic behavior [16,17,28]. In order to compare the rate-sensitive behaviors of these PUUs, the DMA measurements were extended to determine the frequency dependent shifts in their viscoelastic behaviors. Fig. 5 shows the storage modulus curves at 1 Hz and 50 Hz for the PUU 3-2-1 2k and the PUU 2-1-1 1k materials, which have comparable HS contents. The increase in frequency results in the storage modulus curves shifting to the right causing an increase in modulus at any given temperature. This increase in modulus is governed by the rate at which the various viscoelastic transitions shift and the evolving shape of the storage modulus curve with increasing rate/frequency. The shift in $T_{g,s}$ is of particular importance here since it primarily governs the room temperature mechanical behavior due to its proximity. Fig. 5

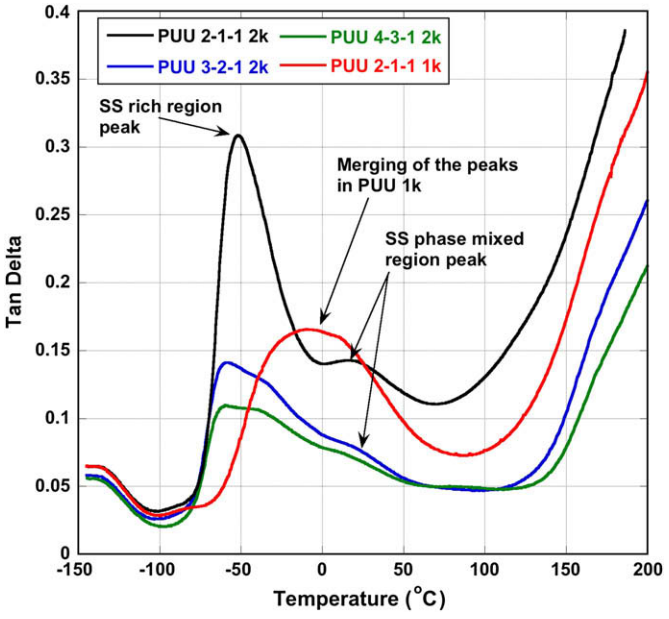

Fig. 4. Plots of tan δ as a function of temperature for the four materials.

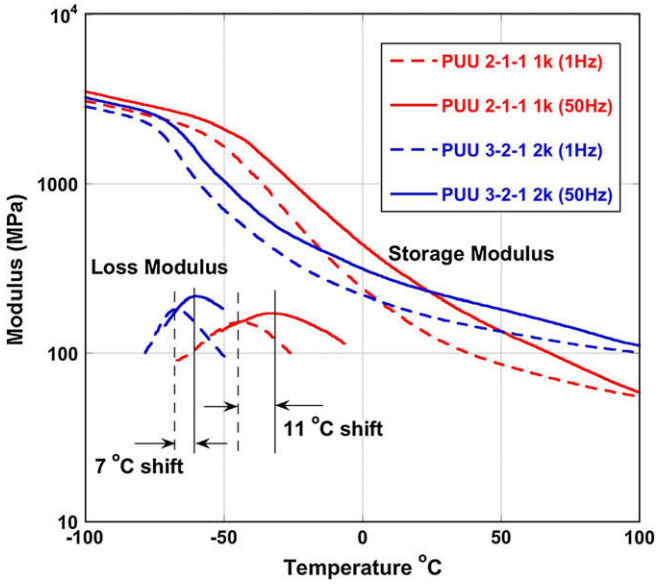

Fig. 5. DMA curves at 1 Hz and 50 Hz for the PUU 3-2-1 2k and PUU 2-1-1 1k.

also shows the loss modulus peaks of the $T_{g,s}$ for the two materials at the two frequencies. The $T_{g,s}$ for the PUU 2-1-1 1k clearly demonstrates a greater shift (~11 °C) than the PUU 3-2-1 2k (~7 °C), indicating a lower activation energy for the 1k material. Table 3 lists the $T_{g,s}$ values (determined from the DMA loss modulus data) at frequencies of 1 Hz, 10 Hz and 50 Hz for all the materials. These frequencies are equivalent of loading the materials at strain rates[2] of $\sim 4 \times 10^{-3}$, 4×10^{-2} and 2×10^{-1} s^{-1}, respectively. On an average, the $T_{g,s}$ for the PUU 2k samples shifts by ~4 °C per decade of strain rate, and is nearly the same for all of them. But for the PUU 1k material, the shift is nearly 7–8 °C per decade of strain rate, almost twice that of the 2k materials. These rates of shift correspond to apparent activation energies of ~203 kJ/mol and ~161 kJ/mol for the 2k and 1k materials, respectively. Hence, at a given temperature, increasing the strain rate by a certain amount will result in a comparatively greater increase in the modulus in the 1k material than in the 2k material. This in addition to the steeper rise in the modulus for the PUU 2-1-1 1k, due to the shape of its storage modulus curve (see Fig. 5) predicts that the 2-1-1 1k material will exhibit a substantially greater rate-dependent stiffening than the 2k material due to the greater phase mixing and increased intermolecular interactions.

4. Rate-dependent stress–strain behavior

To confirm the predictions of the DMA results, the stress–strain behaviors of these PUUs were examined over a range of low and high strain rates.

4.1. Experimental techniques

4.1.1. Quasi-static tests

The samples were tested under uniaxial compression at low strain rates using a Zwick screw-driven mechanical tester at the MIT Institute for Soldier Nanotechnologies (ISN). These tests were performed at strain rates ranging from 10^{-3} to 10^{-1} s^{-1}, under conditions of constant nominal strain rate. The samples were also unloaded at the same strain rate to examine the recovery of the elastic deformation and gauge the permanent set deformation. A single set of uniaxial tension tests was also performed at a strain rate of 10^{-3} s^{-1} to compare against the compressive tests.

4.1.2. High strain rate tests

Samples were also tested under uniaxial compression at high strain rates in the range of 10^3 to 10^4 s^{-1}, using a split Hopkinson pressure bar (SHPB) at the MIT-ISN. The bars were made of aluminum, and the incident and transmission bar were each of 19.75 mm diameter and 2.9 m length; the striker bar was of 51 cm length. A range in strain rates was accomplished by varying the striker bar impact velocity. The complete details of SHPB testing procedures for polymeric materials can be found in [29,30]. Fig. 6 shows a sample high rate stress–strain curve for the PUU 4-3-1 2k obtained using the SHPB. The figure shows the engineering (nominal) stress–strain curve, and the same curve in true stress–strain format. Also included are the engineering strain rate and true strain rate histories during the test. As is observed, the nominal strain rate remains relatively constant during the test, but the true strain rate progressively increases with increasing strain. Due to the large strains attained during these tests, henceforth, the stress–strain curves will be presented in true stress–strain format only. To help identify these curves, each will be identified by an 'average strain rate', an approximate true strain rate reached at half the total true strain of the test.

4.2. Results

4.2.1. Stress–strain behavior under uniaxial compression

The stress–strain curves for the four materials over the entire range of strain rates (10^{-3} to 10^4 s^{-1}) are shown in Fig. 7A–D. The stress–strain curves are seen to be highly nonlinear and rate dependent. The curves are initially linear and relatively stiff followed by rollover to a more compliant behavior. With increasing strain, the stress levels increase as the curves exhibit strain hardening due to increasing orientation of the polymer chains at large strains. Additionally, the stress levels also increase with increasing strain rate. The nature of the stress–strain curves observed here is

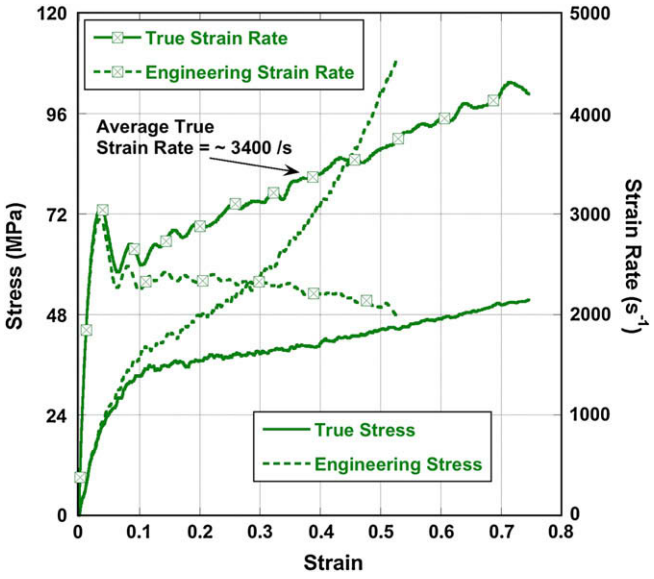

Fig. 6. A sample high rate stress–strain curve for the PUU 4-3-1 2k.

[2] Following Mulliken and Boyce [28], the strain rate is estimated from the test frequency using the relation: strain rate = $(\dot{\varepsilon})$ = (strain/time) = $(d_0/L_g)/(\omega/4)$, where d_0 is the displacement amplitude, L_g is the specimen gauge length and ω is the test frequency.

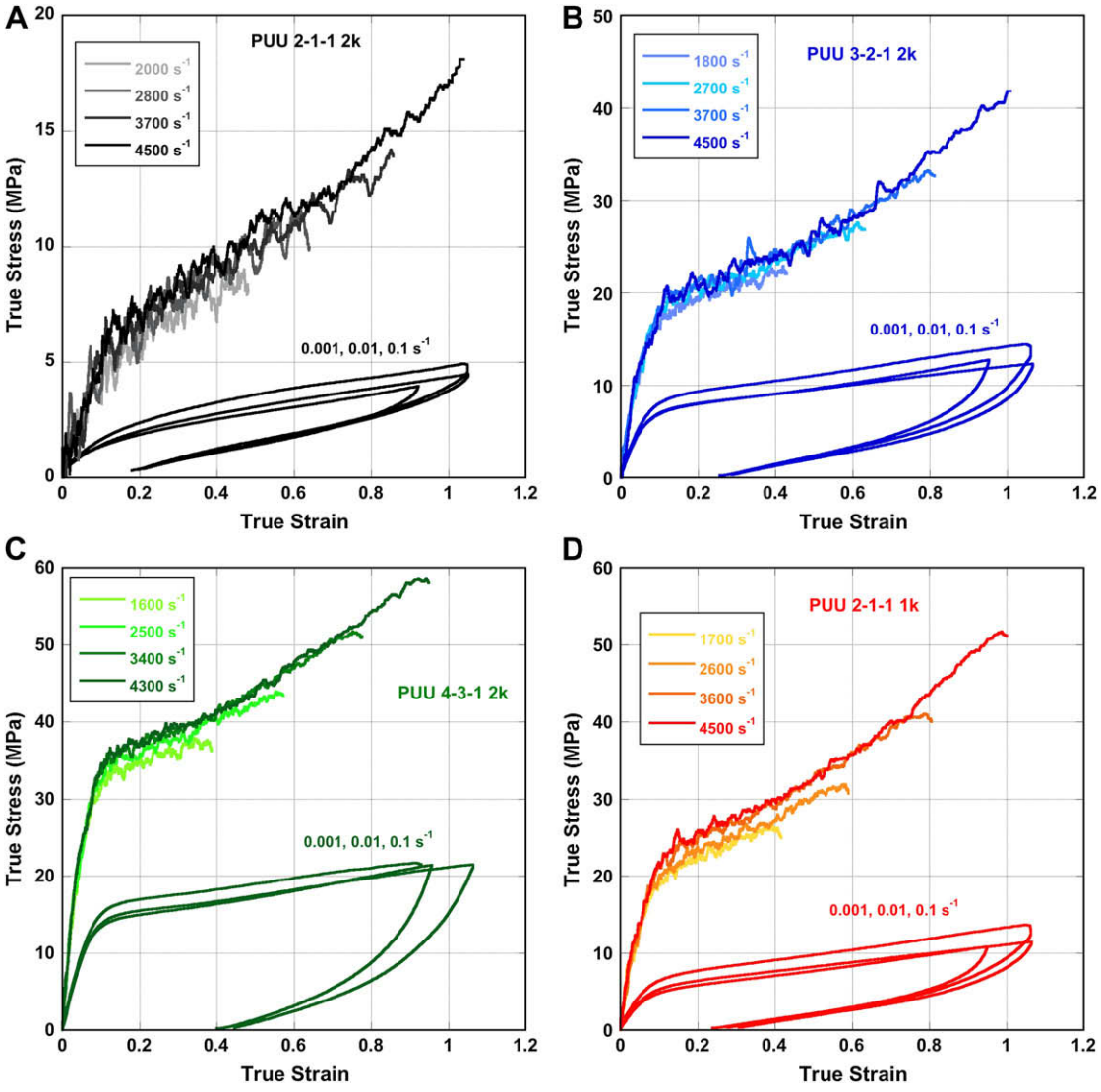

Fig. 7. Compressive stress–strain curves for the PUU materials at various low and high rates (note that for the SHPB data, end points of the curve indicate the end of test and do not represent failure).

similar to those observed for polyurethanes and polyurea by Yi et al. [16] and Sarva et al. [17]. Fig. 7A shows that for the entire set of PUU 2-1-1 2k curves, the flow stress levels are in the 2–20 MPa range, demonstrating a very compliant behavior for this material. Fig. 7B and C show the stress–strain curves for the PUU 3-2-1 2K and the PUU 4-3-1 2K materials. As the HS content is raised, the flow stress values are observed to correspondingly increase. For the 4-3-1 2k, the flow stress values are seen to reach a 15–60 MPa range. This increase in flow stress values for the 2k materials is consistent with the increase in storage modulus that was observed during DMA. Also, as the HS content is increased, the stress–strain curves show sharper transition from the initial linear regime to the region of flow. Fig. 7D shows the stress–strain curves for the PUU 2-1-1 1K material, which shows great rate sensitivity with its curves spanning a 5 MPa–50 MPa range.

For a more precise comparison of the nature of the stress–strain curves, the curves for the four materials at a low strain rate ($10^{-3}\,s^{-1}$) and a high strain rate ($\sim 4500\,s^{-1}$) are shown in Fig. 8. The low rate curves in Fig. 8A clearly show the magnitude of increase in the stress levels with the increase in HS content in the PUU 2k materials. It is interesting to note that the inelastic strain following recovery (permanent set deformation) successively increases with the HS content. PUU 4-3-1 2k exhibits the greatest permanent set deformation. This is presumably due to an irreversible disruption of the interconnected HS domains, as previously suggested by Abouzahr et al. [6]. Fig. 8A and B also show the stress–strain curves for the PUU 2-1-1 1k. At low strain rate, in comparison to the PUU 3-2-1 2k, the PUU 2-1-1 1k has much lower stress levels. But at high strain rate (see Fig. 8B) the stress levels for the 2-1-1 1k are visibly higher. This confirms the trend observed in the DMA data which predicted a significantly greater rate-depending stiffening for the 2-1-1 1k due to its microstructure with greater phase mixing. To accurately gauge the trends in rate sensitivity, the flow stress values for the PUU materials are plotted against strain rate on a logarithmic scale in Fig. 9; the flow stress values in the figure are those attained at 0.3 true strain.[3] At high rates, the flow stress values exhibit a marked increase. The comparatively greater strain

[3] At this strain level, the stress–strain curves have rolled over to flow and are devoid of any significant strain hardening effects. Also dynamic equilibrium has been achieved for the high rate tests at this strain [17].

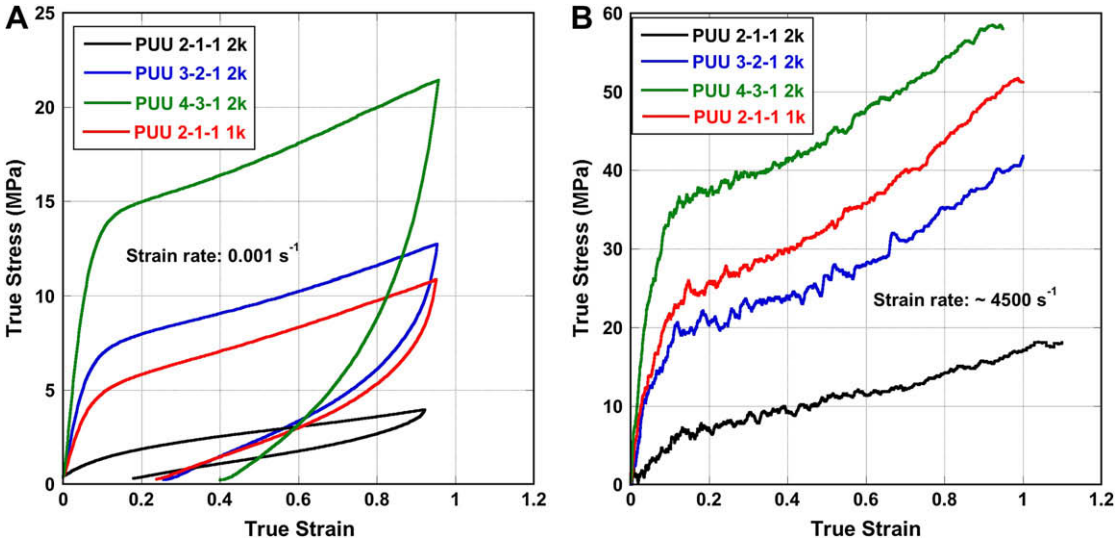

Fig. 8. A comparison of stress–strain curves for the PUU materials at a low (A) and high strain rate (B).

rate sensitivity for the PUU 2-1-1 1k is evident. In the low rate range, the flow stress values for the 2-1-1 1k are lower than the 3-2-1 2k by ~2 MPa, but at high rates they are higher by ~5 MPa. This behavior exhibited by the 2-1-1 1k, where it is more compliant under static loading conditions, but exhibits greater strengthening at high rates, is highly desirable for a range of impact resistant applications. Such properties can help provide rapid and complete unfolding capabilities that are critical during normal use for articles such as face masks and concurrently provide improved protection under impact.

4.2.2. Stress–strain behavior under uniaxial tension

Fig. 10 shows a comparison of the stress–strain curves for the materials under uniaxial tension at a low rate of 10^{-3} s^{-1} (note that these tests were terminated prior to the ultimate failure). The stress levels in tension at large strains are significantly greater than those under compression due to increased strain hardening. In tension, the polymeric chains align in an uniaxial direction along the axis of elongation, compared to a biaxial manner in a plane normal to the loading direction under compression. This leads to a greater orientation induced stiffening in tension. Interestingly, at large strains, the curves for the PUU 2-1-1 1k show a greater stiffening than the PUU 3-2-1 2k. This leads to the PUU 2-1-1 1k manifesting lower stress levels at low strains but higher stresses at large strains (notice the crossover of the 2-1-1 1k and 3-2-1 2k curves at 0.85 true strain). The increased phase mixing, which helps to increase the rate sensitivity in 2-1-1 1k material, also helped improve its strain hardening behavior.

5. Summary

Elastomeric-segmented PUUs are finding increasing usage in applications for protection against impact and blast loadings. To

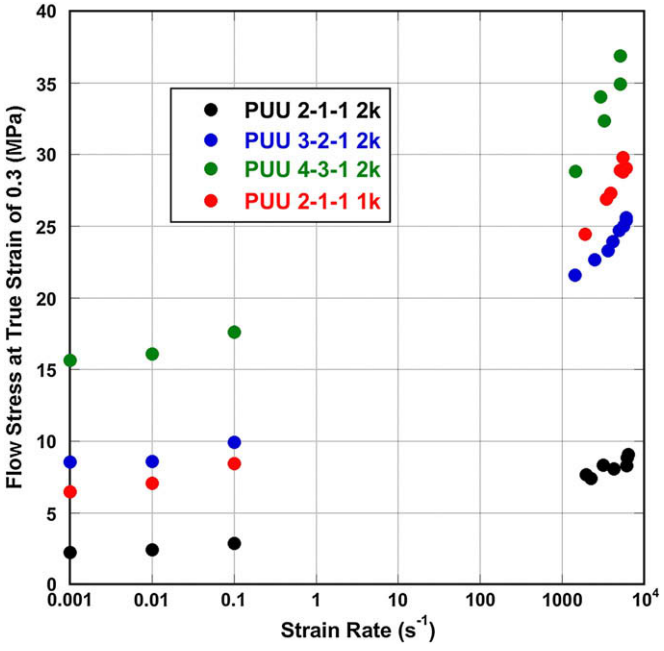

Fig. 9. Flow stress values for the PUU materials at low and high strain rates.

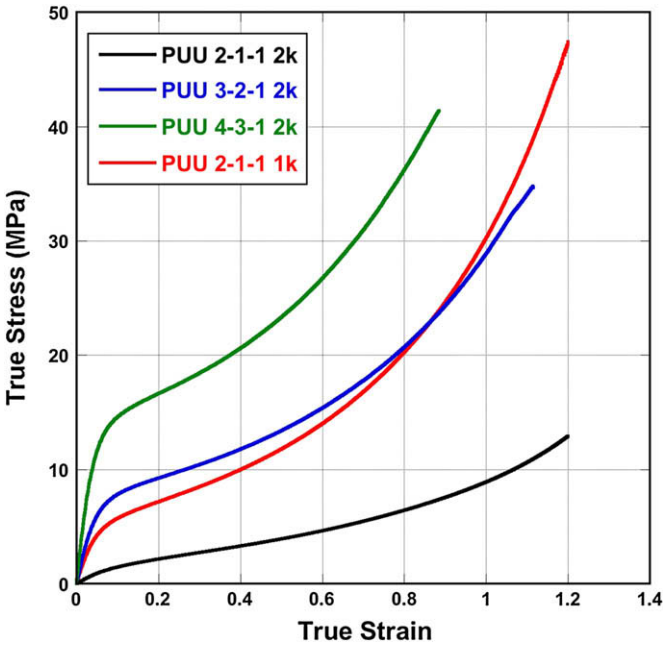

Fig. 10. Stress–strain curves under uniaxial tension for the PUU materials.

help improve impact resistance at high strain rates, it is necessary to build PUUs that are highly rate sensitive and exhibit greatly increased strengths under impact. In this study, we examined PUU materials with varying compositions to examine the mechanisms that govern the overall rate-sensitive mechanical behavior. The microstructures of these model PUUs were examined via SAXS and their mechanical behaviors were investigated via dynamic mechanical analysis, low strain rate compression and tension tests and high strain rate SHPB compression tests.

When the HS content was increased to ~28 wt%, the SAXS data indicated a corresponding increase in the HS interdomain spacing. As the HS content was increased to above ~35 wt%, the SAXS scattering peak broadened and became less distinct due to a greater interconnecting of the HS domains. DMA results showed that, as expected, the rubbery plateau modulus increased with increasing HS content. Consistent with the DMA observations, the mechanical tests showed that with increasing HS content, the stress–strain curves showed an increase in the initial stiffness and the flow stress values at all strain rates. This increase in stress values, however, was accompanied by an increase in permanent set deformation. Hence, though increasing the HS content helped to improve the strength, it also resulted in a decrease in flexibility of the material and hampered its recovery after deformation.

Altering the SS molecular weight (from 2000 g/mol to 1000 g/mol) was observed to promote phase mixing and increase the intermolecular interactions via hydrogen bonds between the hard and soft segments in the material. This change in material microstructure altered its viscoelastic behavior. Specifically, its $T_{g,s}$ and $T_{g,h}$ shifted towards each other, the nature of its storage modulus curve changed such that it exhibited a greater rise in modulus with decreasing temperature, and its $T_{g,s}$ displayed a greater rate/frequency dependent shift. These changes helped greatly improve the rate sensitivity in the material with 1000 g/mol SS MW, such that it showed more compliant behavior at low strain rates, but significantly higher stiffening at high rates. This behavior is highly desirable for a host of applications, where the material is required to possess good flexibility and unfolding capabilities during normal use but also provide improved protection under impact.

In summary, this study examines the effect of microstructure of segmented PUUs on their rate-sensitive mechanical behavior. Insights provided by structural and thermal characterization are corroborated by specialized mechanical tests accessing a wide range of strain rates (10^{-3} to $10^{4}\,s^{-1}$). It is conclusively demonstrated that controlling the phase mixing is key to improving the material performance for high rate applications such as transparent armor.

Acknowledgements

This research was supported by the U.S. Army through the Institute for Soldier Nanotechnologies, under Contract W911NF-07-D-0004 with the U.S. Army Research Office. Alex J. Hsieh acknowledges the PUU materials provided by Dr. Norman Rice of Triton Systems, Inc. through an ISN 6.2 project funded by the Army. AJH also thanks Dr. Rick L. Beyer of Army Research Laboratory for providing assistance with the SAXS and WAXS measurements, and Dr. Shawna M. Liff of ISN for assistance with the tensile tests.

References

[1] Holden G, Legge NR, Quirk R, Schroeder HE. Thermoplastic elastomers. 2nd ed. Cincinnati: Hanser/Gardner; 1996 [chapter 2].
[2] Aneja A, Wilkes GL. Polymer 2003;44:7221–8.
[3] Samuels SL, Wilkes GL. J Polym Sci, Part C, Polym Symp 1973, Battelle Seattle Res Cent 1972;43:149–78.
[4] Lee HS, Yoo SR, Seo SW. J Polym Sci Polym Phys 1999;37:3233–45.
[5] Yeh F, Hsiao BS, Sauer BB, Michel S, Siesler HW. Macromolecules 2003;36:1940–54.
[6] Abouzahr S, Wilkes GL, Ophir Z. Polymer 1982;23:1077–86.
[7] Wang CB, Cooper SL. Macromolecules 1983;16:775–86.
[8] Martin DJ, Meijs GF, Gunatillake PA, Yozghatlian SP, Renwick GM. J Appl Polym Sci 1999;71:937–52.
[9] Martin DJ, Meijs GF, Renwick GM, McCarthy SJ, Gunatillake PA. J Appl Polym Sci 1996;62:1377–86.
[10] O'Sickey MJ, Lawrey BD, Wilkes GL. J Appl Polym Sci 2002;84:229–43.
[11] Kaushiva BD, Wilkes GL. J Appl Polym Sci 2000;77:202–16.
[12] Christenson EM, Anderson JM, Hiltner A, Baer E. Polymer 2005:11744–54.
[13] Sheth JP, Aneja A, Wilkes GL, Yilgor E, Atilla GE, Yilgor I, et al. Polymer 2004;45:6919–32.
[14] James Korley LT, Pate BD, Thomas EL, Hammond PT. Polymer 2006;47:3073–82.
[15] Qi HJ, Boyce MC. Mech Mater 2005;37(8):817–39.
[16] Yi J, Boyce MC, Lee GF, Balizer E. Polymer 2006;47:319–29.
[17] Sarva SS, Deschanel S, Boyce MC, Chen W. Polym Commun 2007;48:2208–13.
[18] Hsieh AJ, Yi J, Pate BD, Boyce MC. 25th army science conference, Orlando, FL; 2006.
[19] Bahei-El-Din YA, Dvorak GJ, Fredricksen OJ. Int J Solid Struct 2006;43:7644–58.
[20] Bogoslovov RB, Roland CM, Gamache RM. Appl Phys Lett 2007;90(22):221910–2.
[21] Roland CM, Twigg JN, Vu Y, Mott PH. Polymer 2007;48(2):574–8.
[22] Grove CM, U.S. Army Edgewood Research Development & Engineering Center Tech. Report; 1999, ECBC-TR-043.
[23] Hsieh AJ, Sarva SS, Rice N. 26th army science conference, Orlando FL; 2008.
[24] Hsieh AJ, Beyer RL, Unpublished data.
[25] Ferry JD. Viscoelastic properties of polymers. 3rd ed., New York: John Wiley & Sons; 1980 [chapter 11].
[26] Sperling LH. Introduction to physical polymer science. New York: John Wiley & Sons; 1986.
[27] Kojio K, Nakashima S, Furukawa M. Polymer 2007;48:997–1004. 2005;46(23):10158–66.
[28] Mulliken AD, Boyce MC. Int J Solid Struct 2006;43:1331–56.
[29] Chen W, Lu F, Frew DJ, Forrestal MJ. J Appl Mech 2002;69:214–23.
[30] Gray III GT, Blumenthal WR. ASM handbook, mechanical testing and evaluation. 10th ed., vol. 8. Materials Park, Ohio: ASM International; 2000. p. 488–96.